Magnetic Dynamics of $Zn^{57}Fe_2O_4$ Nanoparticles Dispersed in a ZnO Matrix

Gerardo F. Goya

***Abstract*—The magnetic properties of diluted $ZnFe_2O_4$ nanoparticles with nearly normal spinel structure, dispersed in a nonmagnetic ZnO matrix, are presented. A magnetic transition to an ordered state is observed at about 19 K, from Mössbauer and magnetic measurements. Detailed characterization of the frequency and field dependence shows that, below the magnetic transition, the system displays several features that suggest a collective freezing of ferrimagnetic particles. Although single-domain particles are inferred from structural data, a dynamic study of this transition hints toward a spin-glass-like process, with $T_g = 17.0(4)$ K and critical parameters $z\nu = 20 \pm 2$, much higher than those of canonical spin glasses. Some facets of these large critical parameters in fine-particle systems are discussed.**

***Index Terms*—Magnetic materials, magnetic semiconductors, Mössbauer spectroscopy, powdered magnetic materials.**

I. Introduction

GRANULAR composites have a wide range of technological applications because their magnetic and electric properties can be tailored for specific applications by choosing appropriate magnetic phases and controlling the particle size and distribution over the nonmagnetic matrix. Practical uses include magnetoresistive sensors [1], high-coercivity [2], and high-permeability materials [3]. Intense experimental work has been aimed toward the description of the transition from the paramagnetic to the frozen state. For extremely diluted fine-particle systems, this transition has been successfully described in terms of a simple superparamagnetic (SPM) model but, as the concentration of magnetic phase is increased, the SPM behavior changes to some different regime where collective freezing of the magnetic moments plays a fundamental role. In order to explain several "anomalous" properties such as field and/or frequency dependence of the transition temperature, the picture of a spin-glass-like (SGL) transition is usually invoked, although the resemblance to a true spin glass (SG) may be wobbly. Only for a concentrated Fe–C nanoparticle system, clear evidence of a SG phase transition through dynamic scaling analysis has been provided [4]. In this work, we show that the magnetic behavior of diluted, single-domain $ZnFe_2O_4$ particles cannot be simply interpreted in terms of a thermally activated Arrhenius–Néel picture for SPM. Instead, the magnetic dynamics of the system displays several SG features, although with extremely high critical parameters.

Manuscript received February 11, 2002; revised May 21, 2002. This work was supported by Brazilian agencies FAPESP and CNPq under Grants 01/02598-3 and 300569/00-9.

The author is with the Instituto de Física, Universidade de São Paulo, CP33618 São Paulo, Brazil (e-mail: goya@if.usp.br).

Digital Object Identifier 10.1109/TMAG.2002.803204.

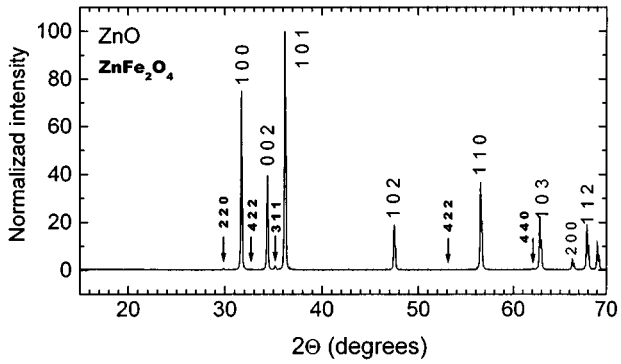

Fig. 1. X-ray diffraction pattern of $Zn_{0.99}{}^{57}Fe_{0.01}O$ sample. The (hkl) numbers for each line are also shown. The arrows indicate the positions of the observed (hkl) reflections for the $ZnFe_2O_4$ spinel phase.

II. Experimental Procedure

Samples were prepared by dissolving zinc oxide (99.99%) and metallic ^{57}Fe (enriched to ~97%) in a 0.2 M solution of HNO_3, to obtain a nominal composition $(Zn_{0.99}Fe_{0.01})O$. The precipitate was gently warmed at 100 °C until complete dried, and afterwards fired in air at 500 °C, 750 °C, and 950 °C for 24 h with intermediate grindings. After the last annealing, samples were slowly cooled (1 K/min) to room temperature. X-ray diffraction patterns were collected using Cu–Kα radiation, and the resulting patterns refined by Rietveld profile analysis [5]. Mössbauer spectra were recorded in transmission geometry between 4.2 K and 300 K in constant acceleration mode, calibrating the velocity scale with α–Fe at room temperature. Magnetic measurements were done using a commercial SQUID magnetometer in both zero-field-cooling (ZFC) and field-cooling (FC) modes, between 5 K $\leq T \leq$ 300 K and applied fields up to 70 kOe. Data were corrected for the diamagnetic contribution of the sample holder and for core diamagnetism of the ions. The in-phase $\chi'(T)$ and out-of-phase $\chi''(T)$ components of the a.c. magnetic susceptibility were recorded at frequencies between 10 mHz $< f <$ 1.5 kHz, with a diving field amplitude of 1 Oe.

III. Experimental Results

The X-ray diffraction pattern of the resulting $Zn_{0.99}(^{57}Fe_{0.01})O$ powder was indexed with the ZnO hexagonal structure, space group $P6_3mc$ (Fig. 1), with cell parameters $a = b = 3.250(1)$ Å and $c = 5.210(1)$ Å. Small peaks corresponding to the most intense reflections of cubic (space group Fd3m) $ZnFe_2O_4$ spinel are also observed. Detailed analysis of these lines showed that the full-width at

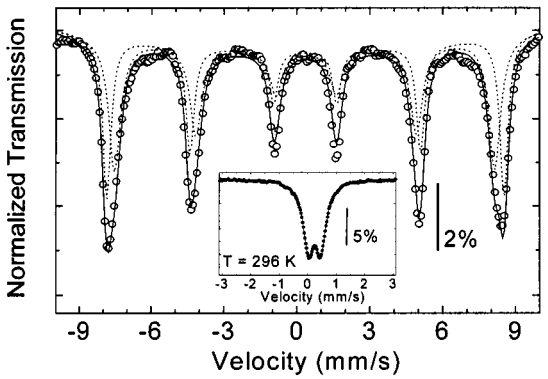

Fig. 2. Mössbauer spectrum (open circles) of $Zn_{0.99}{}^{57}Fe_{0.01}O$ sample recorded at $T = 4.2$ K. Each component of the spectrum (dotted lines), and the total best fit (solid line). Inset: Mössbauer spectrum at $T = 296$ K.

TABLE I
HYPERFINE PARAMETERS

T	B (Tesla)	IS (mm/s)	QS (mm/s)	Γ (mm/s)
4.2 K	48.7(1)	0.45(1)	-0.07(1)	0.50(2)
	50.9(1)	0.44(1)	0.00(1)	0.40(2)
300 K	--	0.35(1)	0.43(1)	0.39(1)

Hyperfine field (B), Isomer shift (IS) quadrupole splitting (QS), and linewidth (Γ) for $ZnFe_2O_4$ phase above and below the magnetic ordering temperature. Errors are quoted between parenthesis.

half-maximum (FWHM) of the three major peaks of the spinel phase, corrected for instrumental broadening was $0.18 \pm 0.04°$, much larger than the corresponding ZnO peaks (FWHM $= 0.06 \pm 0.01°$). Assuming that strain effects do not contribute to the linewidth, an average crystallite size $\langle D \rangle = 23.4 \pm 0.9$ nm was estimated using the Scherrer equation. This indicates that the $ZnFe_2O_4$ phase consists of nanometric particles dispersed in the ZnO matrix, and thus superparamagnetic effects should be expected. When included in the refinement process, the relative amount of the $ZnFe_2O_4$ phase estimated from the profile analysis was $1.1 \pm 0.8\%$, which is in the limit of X-ray detection. The refined cell parameter for the spinel phase was $a = 8.45(1)$ Å.

Mössbauer data taken at $T = 4.2$ K (Fig. 2) show that the system is magnetically ordered, with two subspectra whose hyperfine parameters (see Table I) correspond to the Fe^{3+} oxidation state at tetrahedral (A) and octahedral (B) sites of the $ZnFe_2O_4$ spinel structure [6]. The transition temperature estimated from B *versus* T data (not shown) was $T_{\rm Moss} = 20 \pm 2$ K. At room temperature, Mössbauer spectra displayed a central doublet (inset of Fig. 2) with hyperfine parameters similar to those reported for superparamagnetic $ZnFe_2O_4$ [7], [8]. It is worth to note that the absence of secondary Fe-containing phases (within ~1% of the spectral area) implies an upper limit of <100 ppm for the solubility of iron in the ZnO phase.

Both a.c. susceptibility and ZFC–FC magnetization curves (Fig. 3) show the main SPM features: 1) paramagnetic-like behavior at high temperature; 2) a maximum at $T_f \sim 19$ K which depends on the applied field; and 3) irreversible behavior below ZFC and FC branches below T_f. The temperature of the maximum in $\chi'(T)$, labeled T_f, shifts to higher values with increasing frequencies (upper panel in Fig. 3). This dependence

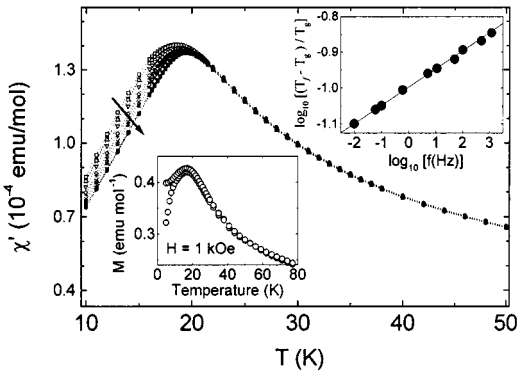

Fig. 3. Main panel: real component $\chi'(T)$ of the ac susceptibility at different driven frequencies from 10 MHz to 1.5 kHz. The arrow indicates the direction of increasing frequencies. Lower panel: dc magnetization curves in ZFC and FC modes near the transition. Upper panel: log–log plot for the reduced temperature $(T_f - T_g)/T_g$ versus external frequency. Solid line is the best fit using (1), with $T_g = 17.0(4)$ K and $z\nu = 20(2)$.

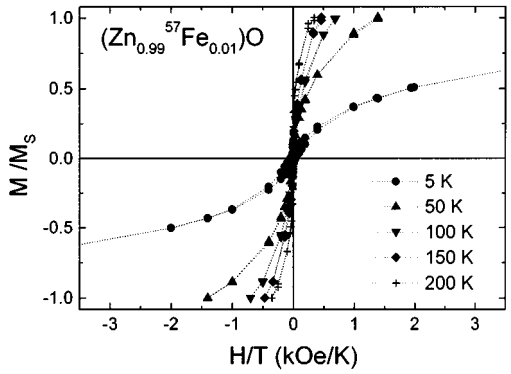

Fig. 4. Reduced magnetization M/M_S versus applied field at several temperatures. Note that the curves do not coalesce even for $T > 10\,T_M$.

will be discussed below. Magnetization versus field curves at different temperatures show that the small coercive field $H_C = 25 \pm 10$ Oe observed above T_f develops steeply for $T < T_f$, up to $H_C = 670 \pm 10$ Oe at 2 K. It can be noted that the system does not saturate even for applied fields of 7 Tesla. However, Fig. 4 shows that there is no superposition of $M(H/T)$ at different temperatures *above* the transition, as expected for a system of noninteracting SPM particles. The saturation magnetization estimated from the high-field region by extrapolation of M versus H^{-1} graphs, $M_0 = 0.14\ \mu_B$/mol $ZnFe_2O_4$ at $T = 2$ K, shows that only a minor amount of atomic moments is uncompensated.

IV. DISCUSSION

The antiferromagnetic transition temperature (T_N) of crystalline $ZnFe_2O_4$ can vary between 9 and 11 K depending on the preparation method. On the other hand, it is well known that a partial migration of Fe atoms from A to B sites yields ferrimagnetic clusters due to the strong A–B superexchange interactions. This partial inversion has been frequently invoked as the source of the much larger T_N observed in $ZnFe_2O_4$ fine particles [6], [9], but it remains unclear whether this is an intrinsic property of nanometric $ZnFe_2O_4$ particles or due to the nonequilibrium chemical routes used for sample preparation, such as sol–gel and mechanical grinding [7]–[9]. Our sample preparation (with a last step of slow cooling to room temperature) yielded spinel

particles with nearly normal spinel structure, as can be inferred from the small saturation magnetization $M_0 = 0.14\ \mu_B$/mol at $T = 2$ K. Assuming that the saturation magnetic moment is only due to Fe at A sites (with $\mu_{Fe} = 5\ \mu_B$), a 0.35 at.% of A-site population is obtained, showing that even for slightly disordered $ZnFe_2O_4$ particles there is an appreciable increase of T_N (at least up to T_f). In any case, the frequency dependence of T_f in our samples indicates that the magnetic transition at this temperature does not correspond to a simple collinear ferrimagnet. On the other hand, although the average linear dimensions (~23 nm) of the present particles are below the single-domain critical diameter (40–80 nm for $ZnFe_2O_4$), the absence of scaling in $M(H/T)$ curves even close to room temperature indicates that other mechanisms in addition to blocking of SPM particles are also operative.

To better clarify the nature of this transition, we attempted to quantify the dependence of the cusp in χ' with frequency through the relative variation in T_f per frequency decade $W = \Delta T_f/(T_f \Delta \log \omega)$ obtaining $W = 0.01$. This value is much smaller than the $W \sim 0.1$–0.13 found in superparamagnets [10], and this smallness yields unphysical results when fitting the data using a thermally activated (Arrhenius) SPM model. On the other hand, the $W = 0.01$ value is somewhat larger than those reported ($\sim 5 \times 10^{-3}$) for canonical spin-glasses [11]. To further check this results, the $\chi'(T, \omega)$ data were analyzed using a conventional critical slowing down model, which states that near the spin glass transition the characteristic relaxation time ($\tau = f^{-1}$) of individual magnetic moments will show a slowing down obeying a power law

$$f = f_0 \left(\frac{T - T_g}{T_g} \right)^{z\nu} \equiv f_0\, t^{z\nu} \tag{1}$$

where T_g is the SG transition temperature, t is called reduced temperature and $z\nu$ is a dynamic critical exponent. From the T_f values, estimated as the maximum in $\chi'(T)$, the best fit to the experimental data yielded $f_0 = 7.2 \times 10^{19}$ Hz, $T_g = 17.0(4)$ K, and $z\nu = 20 \pm 2$. Attempts to fit the data with values of $z\nu$ and f_0 closer to those typical of SG systems were unsuccessful. Interestingly, dynamic scaling of the imaginary susceptibility $\chi''(T, \omega)$ through the relation $\chi''(T, \omega) = t^{\beta}\, \boldsymbol{F}(\omega t^{-z\nu})$ yielded values of T_g and $z\nu$ very close to those obtained from (1) [12]. Although the T_g value is physically sound, the unusually large values of $z\nu$ and f_0 (compared to conventional three-dimensional spin-glasses) would imply that a true SG transition with $Tg > 0$ does not exist in this system. These "abnormally" large critical parameters have been observed, concurrently with departures of the SPM model, in many nanostructured systems where strong interactions and structural disorder usually coexist [13]. For the present samples, however, structural disorder cannot be invoked as the main source to explain the SGL properties, indicating that a more general mechanism is operative for fine-particle systems in between of the high- and low-concentration limits. As dipolar inter-particle interactions due to particle clustering can provide this class of general interactions in dissimilar systems, a systematic study of the freezing transition at different particle concentrations is now underway.

REFERENCES

[1] M. A. Parker, K. R. Coffey, J. K. Howard, C. H. Tsang, R. E. Fontana, and T. L. Hylton, "Overview of progress in giant magnetoresistive sensors based on NiFe/Ag multilayers," *IEEE Trans. Magn.*, vol. 32, pp. 142–148, Jan. 1996.

[2] K. Tamari, T. Doi, and N. Horiishi, "Magnetic and magnetooptical properties of the Co–γ–Fe_2O_3 perpendicular magnetic-films," *Appl. Phys. Lett.*, vol. 63, pp. 3227–3229, Dec. 1993.

[3] J. S. Lee, K. Y. Kim, T. H. Noh, I. K. Kang, and Y. C. Yoo, "Soft-magnetic properties of Fe–B–M–Cu (M = Hf, Zr, Nb) alloys with nanocrystalline and amorphous hybrid structure," *IEEE Trans. Magn.*, vol. 30, pp. 4845–4847, Nov. 1994.

[4] P. Jonsson, T. Svedlindh, and M. F. Hansen, "Static scaling of interacting magnetic nanoparticle system," *Phys. Rev. Lett.*, vol. 81, p. 3976, 1998.

[5] A. Skthivel and R. A. Young, *DBWS-9006PC, Program for Rietveld Analysis of X-ray Powder Diffraction Patterns*. Atlanta, GA: Georgia Institute of Technology, 1991.

[6] W. Schiessl, W. Potzel, H. Karzel, M. Steiner, G. M. Kalvius, A. Martin, M. K. Krause, I. Halevy, J. Gal, W. Schäfer, G. Will, M. Hillberg, and R. Wäppling, "Magnetic properties of the $ZnFe_2O_4$ spinel," *Phys. Rev. B*, vol. 53, p. 9143, 1996.

[7] G. F. Goya, H. R. Rechenberg, M. Chen, and W. B. Yelon, "Magnetic irreversibility in ultrafine $ZnFe_2O_4$ particles," *J. Appl. Phys.*, vol. 87, p. 8005, 2000.

[8] T. M. Clark and B. J. Evans, "Enhanced magnetization and cation distributions in nanocrystalline $ZnFe_2O_4$," *IEEE Trans. Magn.*, pt. 3, vol. 33, pp. 3745–3747, Sept. 1997.

[9] J. C. Ho, H. H. Hamdeh, Y. Y. Chen, S. H. Lin, Y. D. Yao, R. J. Willey, and S. A. Oliver, "Low-temperature calorimetric properties of zinc ferrite nanoparticles," *Phys. Rev. B*, vol. 52, p. 10 122, 1995.

[10] J. L. Dormann, D. Fiorani, and E. Tronc, "Magnetic relaxation in fine-particle systems," in *Advances in Chemical Physics*, I. Prigogine and S. A. Rice, Eds. New York: Wiley, 1997, vol. XCVIII, pp. 322–331.

[11] G. F. Goya and V. Sagredo, "Spin-glass ordering in $Zn_{1-x}Mn_xIn_2Te_4$ diluted magnetic semiconductor," *Phys. Rev. B*, vol. 64, p. 235 208, 2001.

[12] G. F. Goya, "Nonequilibrium magnetic dynamics of $Zn^{57}Fe_{204}$ nanoparticles," *Appl. Phys. Lett.*, submitted for publication.

[13] J. A. De Toro, M. A. López de la Torre, M. A. Arranz, J. M. Riveiro, J. L. Martínez, P. Palade, and G. Filoti, "Nonequilibrium magnetic dynamics in mechanically alloyed materials," *Phys. Rev. B*, vol. 64, p. 094 438, 2001.